Cloud and rain effects on ALTIKA/SARAL Ka band radar altimeter. Part I: modeling and mean annual data availability

Jean Tournadre, Juliette Lambin and Nathalie Steunou

***Abstract*—The AltiKa project developed by the French Centre National d'Etudes Spatiales is based on a wide-band Ka-band altimeter (35.75 GHz). The technical characteristic of the instrument will offer higher performance both in terms of spatial and vertical resolution that will lead to improved observation of ice, coastal areas, inland waters and wave height. An Indian Space Research Organization satellite, Saral will embark the AltiKa altimeter. The launch is scheduled at the end of 2010. The major drawback of Ka band use is the attenuation of the radar signal by atmospheric liquid water. Clouds and rain effects will thus be a strong constraining factor, because the altimeter link budget imposes an attenuation of less than 3 dB. The impact of rain and clouds on Ka-band altimeter data are analyzed and quantify using an analytical model that compute Altika waveforms in presence of rain or clouds. The results are then used to quantify the waveforms attenuation and distortion as well as the error induced on the altimeter geophysical parameters estimates. Because of the non-linearity of attenuation relations, the impact of clouds/rain depends more on the clouds/rain variability within the altimeter footprint than on the mean characteristics, which makes correction using coincident rain or cloud data difficult. Small rain cell and small dense clouds can thus strongly distort the waveforms and lead to erroneous geophysical parameters estimates. The probability of 20 Hz and 1-sec averaged data loss are computed from the models results and from cloud and rain climatologies. On a global scale, about 3.5% of the 20 Hz data will be lost because of rain and clouds and 2.5% of the 1-sec averaged data. However, the probability strongly varies over the global ocean and can exceed 10% in the Tropics.**

***Index Terms*—Ka-band altimeter, rain and cloud impact, geophysical parameters estimates.**

I. Introduction

SATELLITE radar altimetry is a technique used in oceanography to measure sea level on a large scale. The data obtained are of great importance to understand ocean circulation and its variations. The AltiKa project, developed by the French Centre National d'Etudes Spatiales (CNES), is based on a wide-band Ka-band altimeter (35.75 GHz, 500 MHz bandwidth). It will be the first oceanography altimeter to operate at such a high frequency. This unique technical characteristic of the instrument will offer improvements both in terms of spatial and vertical resolution [1]. The instrument's more accurate measurements should lead to improved observation of ice, coastal areas, inland waters and wave height. An Indian Space Research Organization (ISRO) satellite, Saral (Satellite with ARgos and AltiKa), will embark the AltiKa altimeter, built by CNES.

The one major drawback of Ka band is that attenuation due to liquid water (rain and clouds) in the atmosphere is high. Preliminary studies of Ka band altimeter have shown that light rain can strongly attenuate the radar signal and distort the altimeter echo waveform [2]. Clouds droplets, although their absorption coefficient is on average one order of magnitude smaller than the one of rain drops [3], can also have a significant impact on Ka-band radar signal as shown by [4] and can not be neglected as done for Ku-band altimeters. The Altika altimeter link budget imposes, in the worse case, a limitation of 3 dB on the atmospheric attenuation of the radar signal. This constitutes a strong constraint that will condition the availability of the altimeter data in presence of rain and clouds. It is thus imperative to precisely assess the impact of liquid water on the Altika data and to estimate the data availability which should be above 90% to meet the mission requirements.

Several studies, [5], [6], [7], [8], has been published on the effect of rain on dual-frequency (Ku- and C-band) altimeter data. The model developed by [7] and [2] to compute Ku band altimeter waveforms in presence of rain, can be easily adapted to Ka band and can be used to estimate and analyze the effect of rain and clouds on Altika waveforms (see section 3). The impact of liquid water on the accuracy of the geophysical parameter inferred from waveform analysis is then estimated by applying the planned retracking algorithm to the waveforms simulated in presence of rain and clouds. The results are then synthesized to estimate the probability of high attenuation (larger than 3 dB) and high distortion as a function of rain rate and cloud integrated liquid water content. These probabilities are then used to estimate the probability of data loss using available rain and cloud liquid water climatologies (see section 5).

II. Altika

The main instrument of the Altika/SARAL satellite is the Altika Ka-band altimeter that is derived from the Poseidon altimeter and operates at 35.75 GHz. The satellite payload will also include three other instruments. A dual frequency microwave radiometer (23.8 GHz and 36.8 GHz) embedded in the altimeter and sharing the antenna will provide the data

J. Tournadre is with IFREMER (Institut Français de Recherche pour l'Exploitation de la Mer), Laboratoire d'Océographie Physique et Spatiale, IFREMER, 29280 Plouzané, France, e-mail: jean.tournadre@ifremer.fr

J. Lambin and N. Steunou are with Centre National D'Etudes Spatiales, 31401 Toulouse, France.

necessary to correct the wet troposphere effects. A Doppler Orbitography and Radiopositionning Integrated by Satellite (DORIS) receiver [9] and a Laser Retro-Reflector Array (LRA) constitute the orbitography system that will provide the necessary data for a precise orbit determination. A detailed description of the mission's payload is given in [1].

The SARAL satellite will be positioned on a 35-day repeat period sun-synchronous orbit of 800 km altitude and 97 ^{o} inclination. The altimeter uses an offset-fed reflector antenna of 1 m in diameter, which will have a beamwidth of 0.61 ^{o} (i.e. less than half that of Ku-band altimeters). The Altika bandwidth (500 MHz) will be about 30% higher than that of Ku-band altimeter and will lead to much smaller footprint. The Pulse Repetition Frequency will be 4 KHz, approximately twice that of most conventional altimeters which should imply much smaller instrumental noise.

The mission specifications for the altimeter error budget of the 1-sec averaged (GDR) data products are: 1.5 cm for the altimeter range noise, 0.5 dB on the absolute σ_0 value, 5% or 25 cm for significant wave height (swh).

III. Modeling the impact of cloud and rain on Altika waveform

A. Waveform model

The model of altimeter echo in presence of rain proposed by [7] is based on the work of [10], [11], [12],[13]. It is described in detail in [7] and is here only briefly outlined. The backscatter coefficient, $\sigma(t)$, is expressed as a double convolution product of the radar point target response, the flat sea surface response and the joint probability density function of slope and elevation of the sea surface [10]. The presence of rain or clouds within the altimeter footprint changes the computation by introducing a perturbation in the form of an attenuation of the radar signal, $A_R(u,\theta)$ to every point of the altimeter footprint. Assuming a Gaussian shape for the antenna beam pattern and for the compressed altimeter pulse and a Gaussian joint probability of sea surface slope and elevation, σ is expressed as

$$\sigma(\frac{2x}{c}) = \frac{2\pi H'' \sigma_\tau \sigma_0}{\sigma_p} \int_0^\infty e^{-\frac{u}{u_b}} e^{-\frac{(x-u)^2}{2\sigma_p^2}} \left[\frac{1}{2\pi}\int_0^{2\pi} A_R(u,\theta)d\theta\right] du \quad (1)$$

where u is a variable related to the distance from nadir, $x = ct/2$ is the range, $H'' = H/(1+H/a)$ is the reduced satellite height, a being the earth's radius, and H the satellite height. σ_τ is the standard deviation of the altimeter pulse; $\sigma_p = \sqrt{h^2+\sigma_\tau^2}$ where h is the rms wave height; u_b is the antenna pattern standard deviation; and σ_0 is the surface backscatter coefficient.

The attenuation by rain has been widely studied since the 1940's and the literature on the subject is plentiful. The one-way signal attenuation, k_p (in dB.km^{-1}), is related to the rain rate (in mm.h^{-1}) by the Marshall-Palmer relation [14],

$$k_p = \alpha R^\beta \quad (2)$$

where α and β are frequency dependent coefficients (0.337 and 0.904 [15] [16]). The two-way total attenuation, A_R, depends on the rain height, H_R and on k_p

$$A_R = 10^{-\frac{2H_R k_p}{10}} = 10^{-\frac{1}{5}\alpha H_R R^\beta} \quad (3)$$

Attenuation from cloud coverage depends of the cloud liquid water content l (in g.m^{-3}). The attenuation , k_p (in dB.km^{-1}) is given by

$$k_p = \kappa l \quad (4)$$

where $\kappa = 1.1$ dB km^{-1}/(g.m^{-3}) [13]. The two-way total attenuation, A_R is thus

$$A_R = 10^{-\frac{2H_c k_p}{10}} = 10^{-\frac{1}{5}\kappa L} \quad (5)$$

where H_c is the cloud thickness and $L = l\,H_c$ is the integrated cloud liquid water content (ILWC).

For both raining and non-raining clouds, the attenuation by ice particles has been neglected as it is always at least one order of magnitude smaller than the liquid water one. The attenuation field, A_R, can be estimated from either real data (such as meteorological radar or satellite data) or from analytical cloud/rain models. Three models were used in this study: Gaussian, exponential and constant. A detailed description is given in Appendix.

B. Waveform analysis

The rain/cloud effect on waveforms is estimated through three indicators. The first one measures the attenuation of the signal A_w and is defined by

$$A_w = 10\log_{10}\left(\frac{\max(\sigma(t))}{\max(\sigma_f(t))}\right) \quad (6)$$

where σ_f represents the rain-free waveforms.

The second indicator, which estimates the deformation of the waveform leading edge, is defined as the ratio of the leading edge slopes, *S*, for the rainy and non rainy waveforms.

$$S = \frac{t_{max} - t_{noise}}{t_{fmax} - t_{fnoise}} \quad (7)$$

where the times t_{max} and t_{noise} are defined by:

$$\sigma(t_{max}) = \max[\sigma(t)] \quad (8)$$

$$t_{noise} = \min[t_i;\, \sigma(t_i) >= \max(\sigma(t))/100] \quad (9)$$

The third indicator is the square of the off-nadir angle, ζ^2, as defined in the standard Geophysical Data Record products (GDR) for Jason and Envisat [17]. Using the Brown model [10] of waveform, the estimate the square of the off-nadir, ζ^2, (or mispointing angle) is related to the slope of the logarithm of the trailing edge [17] by

$$\zeta^2 = \frac{1+M}{2(1+2/\gamma)} \quad (10)$$

where γ:

$$\gamma = \frac{4}{2\log 2}\left(\sin\frac{\Psi_b}{2}^2\right) \quad (11)$$

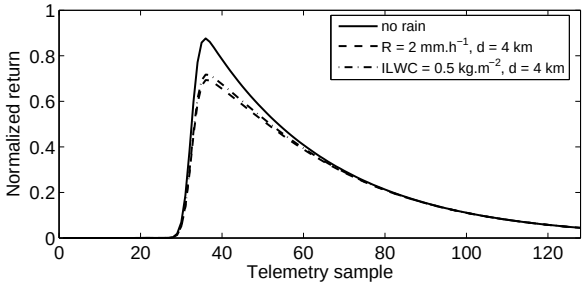

Fig. 1. Altika waveforms modeled in presence of cylindrical rain cell or cloud.

where Ψ_b is the antenna beam width and M is the slope of the plateau estimated by linear regression as

$$\log(\sigma_f) = M(\alpha x) + N \tag{12}$$

with $\alpha = 4\frac{cH''}{\gamma H^2}$. As the computation is based on the slope of the waveform trailing edge, it is a very good indicator of the deformation of the waveform as already shown for Topex waveforms [7]. It should be noted that this estimate can take negative values, which results from modification of the trailing edge not caused by mispointing. In general, by misuse of language, ζ^2 is commonly refer to as off-nadir angle estimate.

C. Modeling of rain and cloud impact on waveforms

In essence the impact of rain and clouds on the Ka band altimeter is similar to the one encountered for Ku band altimeters but attenuation is about ten times larger at Ka band than that at Ku band rendering the problem of rain more constraining. Furthermore, while attenuation by cloud liquid water is weak enough at Ku band (of the order of tenth of dB) to be neglected, at Ka band it is of the same order of magnitude as the light rain one at Ku band and has thus to be taken into account. The waveform model presented in section 3-A is used here to analyze in details the impact of rain and clouds on the Altika waveforms. The modeling results are then used to yield quantitative estimates of the waveforms attenuation and distortion.

The waveform model [1] depends on the significant wave height, SWH, (defined by $SWH = 4h$) and on the distribution of attenuation (A_R) within the altimeter footprint. The tests conducted to study the impact of wave height (not presented here) on attenuation, off-nadir angle and on slope showed that it is almost always negligible, except for very large sea states. It is thus not considered in this study and the modeling is performed using a fixed significant wave height of 2 m (i.e. the mean global wave height).

The attenuation and distortion of Altika waveforms in presence of rain and cloud can be easily seen in Figure 1 which presents the waveforms modeled for a Gaussian cylindrical rain cell of 2.0 mm.h^{-1} rate, 4 km diameter and 1 km height and a Gaussian cloud of 0.5 kg.m^{-2} ILWC, 4 km diameter. The attenuation is 1 dB for the rain cell and 0.86 dB for the cloud, and the off-nadir angle estimates are 3.0 and 3.3 10^{-3}deg^2 respectively.

1) Rain: The impact of rain is modeled using the three analytical models of cylindrical rain cells given in Appendix for a large range of rain rate, cell diameter and rain height. The altimeter waveforms are computed at a 20 Hz rate (i.e. one waveform every 580 m) as the altimeter passes over the rain cell, i.e. for different x_0. For each waveform, attenuation, A_w, off-nadir angle, ζ^2, and slope, *S*, are computed as well as the mean, $\overline{IR}$, and standard deviation, IR_{std}, of the integrated rain rate (product of rain rate and rain height) over the altimeter footprint ($\sim$6 km radius at telemetry sample 104). Figure 2 presents the three parameters for Gaussian rain cells as a function of $\overline{IR}$ and IR_{std} for the 20 Hz waveforms. As previously shown by [7] for Ku band altimeter, attenuation depends both on $\overline{IR}$ and IR_{std}. It increases with increasing integrated rain rate and variability. For integrated rain rate larger than 4 $\mathrm{mm.h^{-1}.km}$, attenuation is always larger than the 3 dB limit causing the loss of the signal. It is always larger than the one that can be estimated from the mean rain rate over the altimeter footprint using the Marshall-Palmer relation [2] and that could be estimated, for example, from coincident radiometer measurements. The difference increases rapidly with increasing rain variability and exceeds 1 dB even for very light rain rates and for IR_{std} larger than 0.5 $\mathrm{mm.h^{-1}.km}$. This underestimation, due to the non-linearity of the attenuation relations, shows that the effects of a rain cell are not linearly related to its dimension and strength and that the correction of backscatter coefficients using coincident rain rate estimates from radiometer data is impossible.

The off-nadir angle depends mainly on IR_{std} and only weakly on $\overline{IR}$, except for very light rain rates. It generally exceeds 0.01 deg^2 for IR_{std} larger than 0.75 $\mathrm{mm.h^{-1}.km}$. The slope of the leading edge depends both on rain rate and rain variability and is strongly modified for small intense rain cells characterized by low rain rates and high variability. Waveforms can thus be strongly distorted even for light rain and low attenuation. In such cases, the retrieval of geophysical parameters would be significantly hampered. It is important to note that rain variability has a much stronger impact on the waveform distortion at low rain rate than that at a higher one. Similar results were found for exponential and constant rain cells but are not shown here.

2) Clouds: The impact of clouds on Ka band altimeter data has been studied only by [4] and [18] which showed that clouds can seriously degrade the altimeter track point precision, i.e. the estimate of range. However, only two cases of clouds were studied and analyzed in terms of altimeter height measurements. In this study, we analyze the impact of clouds for a large range of cloud liquid water content, and diameters using both analytical cylindrical cloud models (see Appendix) and cloud liquid water content measurements from MODIS high resolution (1 km) cloud data (L2 Swath 1km Collection 005 products available at *http://modis-atmos.gsfc.nasa.gov/MOD06_L2/*) [19]. As for rain, the al-

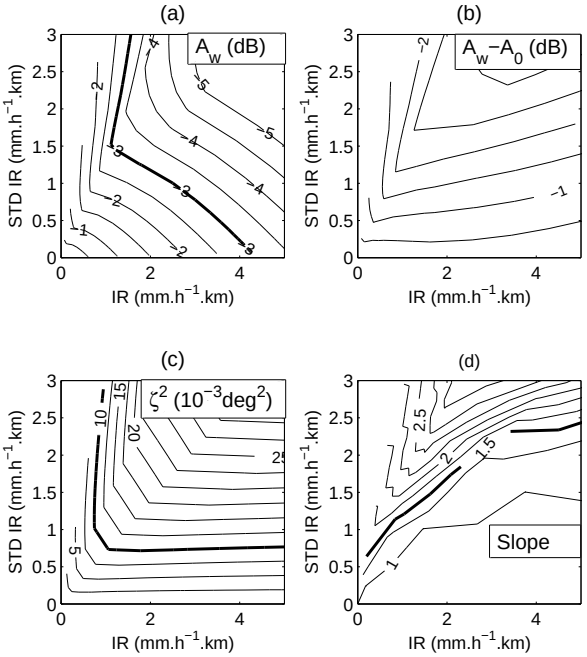

Fig. 2. Modeling of rain impact on Altika 20 Hz waveforms for Gaussian rain cells. Attenuation (in dB) (a), difference between the attenuation and the one estimated from the mean rain rate using the Marshall-Palmer relation (A_0) (b), off-nadir angle (in $10^{-3}\mathrm{deg}^{-2}$) (c) and slope (d).

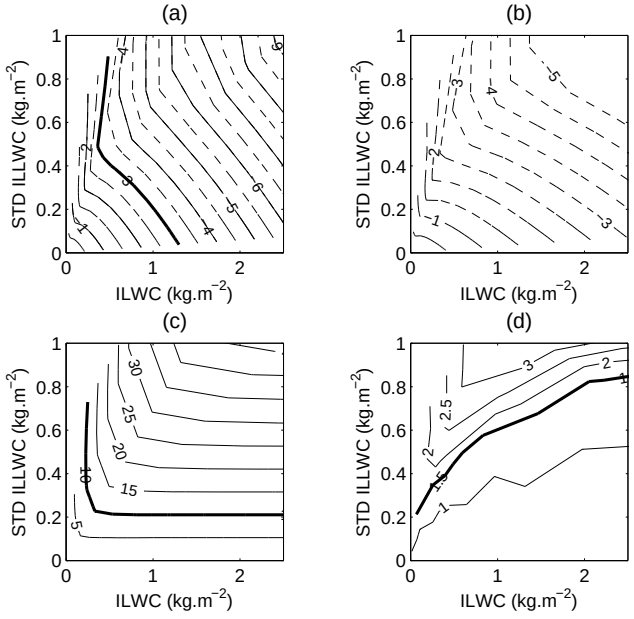

Fig. 3. Impact of Gaussian clouds on 20 Hz Altika altimeter waveforms. Attenuation (a), difference between waveform attenuation and the attenuation estimated from the mean liquid water content (b), off-nadir angle (in 10^{-3} deg^2) (c) and leading edge slope (d).

timeter waveforms are computed at a 20 Hz rate as the altimeter passes over the clouds. For each waveform, attenuation, A_w, off-nadir angle, ζ^2, and slope are computed as well as the mean, $\overline{L}$, and standard deviation, L_{std}, of the ILWC over the altimeter footprint. The results are presented in Figure 3 for Gaussian clouds as a function of $\overline{L}$ and L_{std}. As it could be expected, the distributions are very similar to the rain ones. Attenuation increases with increasing $\overline{L}$ and increasing L_{std}. For $\overline{L}$ greater than 1.2 $\mathrm{kg.m}^{-2}$, it exceeds 3 dB causing the loss of the signal. This attenuation is always larger than the one that can be estimated from the mean ILWC over the altimeter footprint using relation [4] and their difference increases rapidly with increasing rain variability. It exceeds 1 dB even for $\overline{L}$ larger than 1 $\mathrm{kg.m}^{-2}$ and L_{std} larger than 0.1 $\mathrm{kg.m}^{-2}$. The off-nadir angle depends mainly on L_{std} and only weakly on $\overline{L}$. It exceeds 0.01 deg^2 for $\overline{L}$ larger than 0.25 $\mathrm{kg.m}^{-2}$. The slope of the leading edge is weakly sensitive to ILWC but it increases rapidly with rain variability. The waveforms can thus be significantly distorted even for medium to low $\overline{L}$, and the accuracy of the retrieved geophysical parameters can thus, as for rain, be seriously degraded in presence of small dense cloud . Similar results were found for exponential and constant clouds but are not shown here.

IV. Impact on geophysical parameter estimates

The data set of the Ka-band waveforms modeled in presence of rain and clouds is used here to quantify the errors induced by atmospheric liquid water on the geophysical parameters estimated by a retracking algorithm. The ground processing foreseen for the production of Altika Geophysical Data Record, i.e. for the retrieval of the range, surface backscatter, significant wave height and off-nadir angle is the one developed for the Jason-1-Poseidon-2 altimeter reprocessing. This so-called MLE4 algorithm is described in detail in [20]. It uses a second order analytical model of altimeter echo adapted from the classical Brown [10] model and including mispointing (off-nadir) angle effects. The retracking process consists of the estimation of the 4 geophysical altimeter parameters that condition the model echo by fitting the model and observed altimeter echo waveforms using an unweighted Least Square Estimator derived from Maximum Likelihood Estimators. For each modeled Altika waveform the MLE4 estimates are compared to the true values that were used to simulate the waveforms, as well as to the attenuation A_w and off-nadir angle, ζ^2, computed by the waveform analysis presented in section 3.

This comparison is first conducted on the ensemble of waveforms simulated in presence of rain for the three type of rain cells and for the whole range of rain characteristics. The retrieval converges for 99.9% of the waveforms and the Mean Quadratic Error (distance between modeled and measured waveform) is below 5.10^{-4}, i.e. the validity threshold used for Jason-1, for 98% of the cases. Although the waveforms can be strongly modified and distorted, the retracking algorithm performs almost always nominally and can thus not be used to identified the data potentially affected by rain.

The mean bias and standard deviation of the geophysical parameters have been computed as a function of rain char-

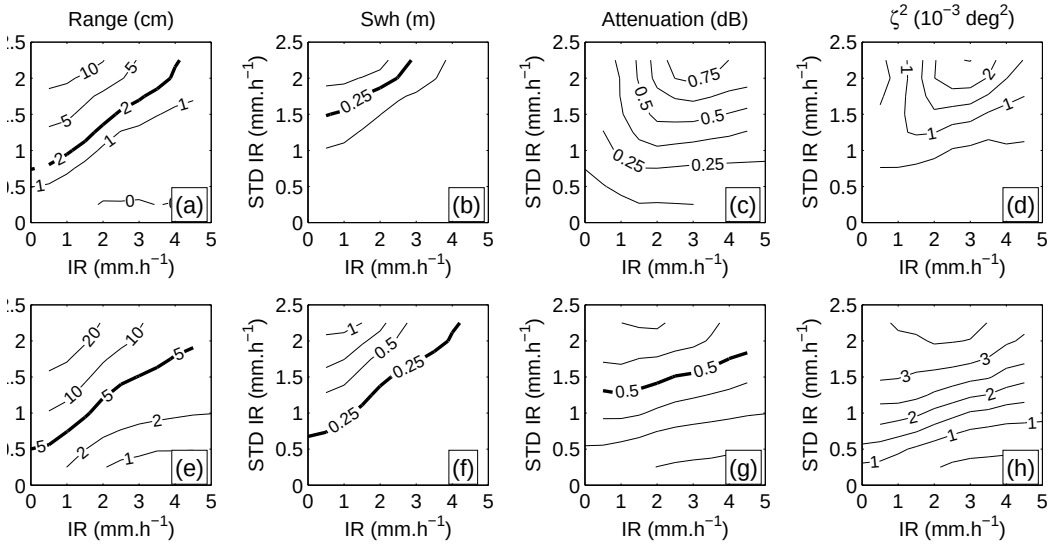

Fig. 4. Mean biases (a to d) and standard deviations (e to h) of the geophysical parameter estimates as a function of mean and standard deviation of the integrated rain rate within the altimeter footprint; MLE4 and true range (cm) (a and e), MLE4 and true significant wave height (m) (b and f), MLE4 and apparent backscatter (dB) (c and g) and MLE4 and measured off-nadir angle (10^{-3} deg^2) (d and h).

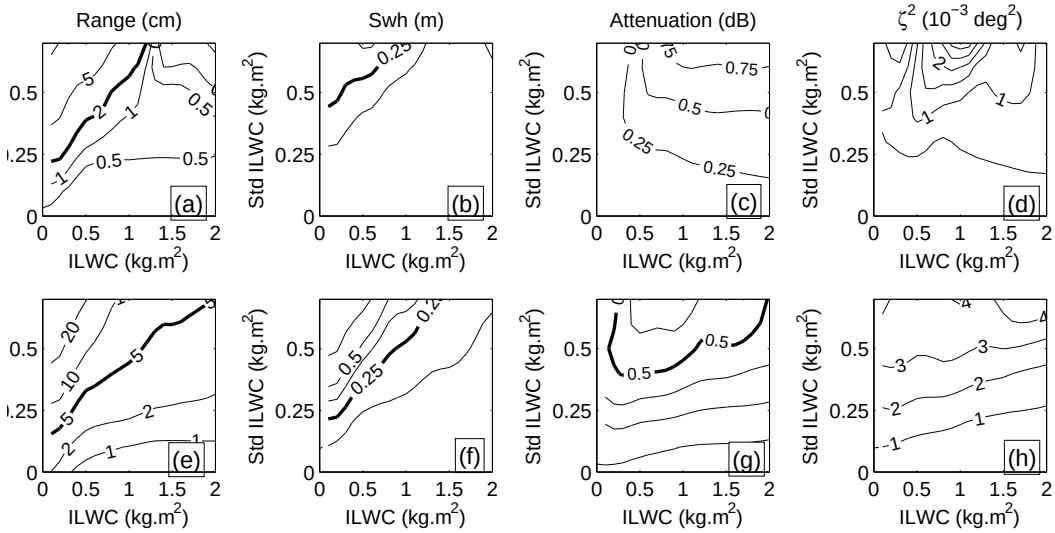

Fig. 5. Mean biases (a to d) and standard deviations (e to h) of the geophysical parameter estimates as a function of mean and standard deviation of the integrated cloud liquid water within the altimeter footprint; MLE4 and true range (cm) (a and e), MLE4 and true significant wave height (m) (b and f), MLE4 and apparent backscatter (dB) (c and g) and MLE4 and measured off-nadir angle (10^{-3} deg^2) (d and h).

acteristics, i.e. the mean and standard deviation of integrated rain rate within the altimeter footprint by binning the data by classes of 0.2 $\mathrm{mm.h^{-1}.km}$. Figure 4 synthesizes the results of this analysis. The range estimate (see Figures 4-a and -e) and the swh one (see Figures 4-b and -f) are very sensitive to waveform distortion, especially to the modification of the leading edge slope as shown by the similarity of the std patterns and the leading edge slope distribution presented in Figure 2-d.

For small intense rain cells associated to high rain variability, the strong modification of the leading edge cannot be correctly modeled by MLE4 and results in high range and swh biases and standard deviation. The mean bias and std increase rapidly with rain variability (and weakly with rain rate). The bias exceeds 2 cm for range, 10 cm for swh while the std exceeds 5 cm for range and 25 cm for swh for rain variability larger than 0.5 $\mathrm{mm.h^{-1}.km}$. For homogeneous rain cells, i.e. for low rain variability, the leading edge is weakly modified (see Figure 2-d) and MLE4 performs much better which translates to a smaller bias and std for both range and SWH. The bias remains below 2 cm for range and below 25 cm for swh while the std is lower than 5 cm for range and 25 cm for swh, i.e. within the sensor's performance specifications. In presence of rain, the retrieval of the true surface backscatter using any kind of retracking algorithm such as MLE4 is impossible because the model does not include any attenuation by atmospheric

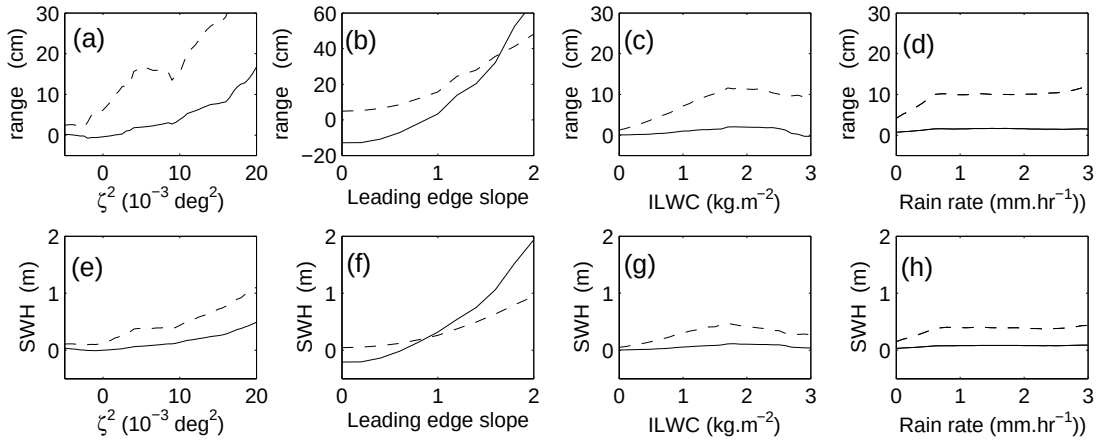

Fig. 6. MLE4 range and swh biases (solid lines) and standard deviations (dashed lines) as a function of waveform off-nadir angle (a and e), leading edge slope (b and f), ILWC (c and g) and rain rate (d and h).

liquid water. The algorithm can thus not possibly correct atmospheric attenuation and can only estimate an apparent backscatter that is the true surface backscatter minus the atmospheric attenuation. The comparison of the true and MLE4 backscatter is useless but it is important to test the ability of MLE4 to estimate at least the true apparent backscatter as computed by waveform analysis. As shown in Figure 4-c and -g, MLE4 overestimates the apparent backscatter and the bias increases with rain variability and rain rate from about 0.25 dB for low rain variability ($<1\ \ \mathrm{mm.h^{-1}.km}$) to more than 0.5 dB for large rain variability ($>1.5\ \ \mathrm{mm.h^{-1}.km}$) and large rain rate ($>2\ \ \mathrm{mm.h^{-1}.km}$). Indeed, the modification of the slope of the waveform plateau by rain attenuation resembles the effect of mispointing although the principle is in essence different. The inversion of the rain/cloud affected waveforms by MLE4, which includes mispointing effects, results in non zero off-nadir estimates and thus in an overestimation of the backscatter. It is also useless to compare the true (fixed to 0) and MLE4 off-nadir estimates, i.e. the off-nadir error, but it is important to test the ability of MLE4 to correctly estimate the variation of the slope of the waveform plateau induced by rain. The results of this comparison presented in Figure 4-d and -h show that MLE4 performs very well in retrieving the plateau slope as the bias is almost negligible ($< 3\,10^{-3}\mathrm{deg}^2$) as well as the standard deviation ($< 4\,10^{-3}\ \mathrm{deg}^2$).

The results of the same analysis performed for waveforms in presence of clouds, presented in Figure 5 are very similar to the ones found for rain. The range and swh biases and standard deviation depend mainly on the modification of the leading edge slope, as can be easily seen by comparison of Figure 5-a, -b, -e and -f to Figure 3-d). Their values exceed the performances specifications for small dense clouds with high ILWC variability. For homogeneous clouds, MLE4 performs well and the bias and std remains small. For the apparent backscatter and off-nadir angle, the results are identical to the rain cases, with an overestimation of the true apparent backscatter and a very good estimation of the slope of the plateau. The accuracy of the MLE4 retrieved range and swh degrades when the waveforms are distorted especially when

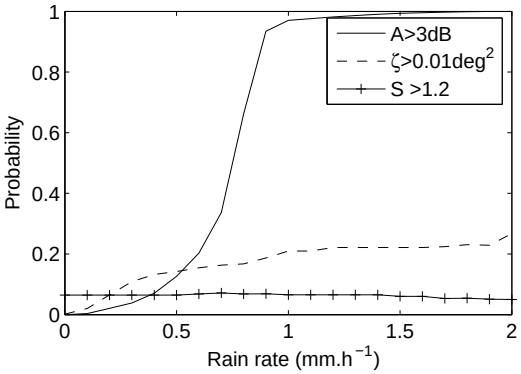

Fig. 7. Probability of attenuation exceeding 3 dB (a), of off-nadir angle exceeding 0.01 deg^2 (b) and of slope exceeding 1.2 (c) as a function of rain rate.

the slope of the leading edge is significantly modified. These situations correspond mainly to cases where the rain or ILWC variability is high, such as in small intense rain cells or small dense clouds that are difficult to accurately detect using coincident microwave radiometer data. This can be easily seen in Figure 6 which presents the mean range and swh bias as a function of off-nadir angle, leading edge slope, rain rate and ILWC. The range and swh biases and std rapidly increase with leading edge slope and off-nadir angle. For off-nadir angles larger than 0.01 deg^2 and for leading edge slopes larger than 1.2, the bias exceeds 2 cm and the standard deviations 10 cm, which largely exceeds the performance specifications. The range and swh biases and standard deviations are only weakly dependent on rain rate and ILWC which confirms that a flag based uniquely on coincident rain or ILWC measurements can not perform correctly and that it will be necessary to develop an independent rain/cloud flag based on the altimeter measurement itself to detect the samples that will be weakly affected by rain and clouds.

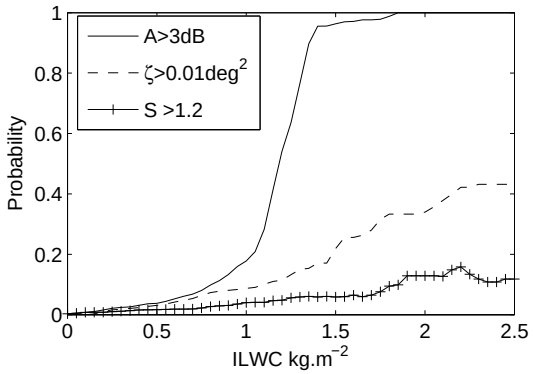

Fig. 8. Probability of attenuation exceeding 3 dB (a), of off-nadir angle exceeding 0.01 deg^2 (b) and of slope exceeding 1.2 (c) as a function of Integrated Cloud liquid water Content.

V. Availability of Altika data

The technical characteristics of the instrument and the analysis of the geophysical parameters errors show that Altika data will be either lost or too strongly affected if the attenuation is larger than 3 dB, the off-nadir angle larger than 0.01 deg^2 and the leading edge slope larger than 1.2. These limits will constrain the availability of the Altika measurements. The results of the modeling are here used to estimate this availability from precipitation and cloud climatologies.

A. Availability of 20 Hz Altika data

As only rain rates are available in rain climatology, the probabilities of high attenuation and distortion of 20 Hz Altika data have been computed as a function of rain rate by synthesizing the results of the ensemble of simulations for all types of rain cells (Gaussian, exponential, constant) and characteristics (rain rate, diameter, rain height). They are presented in Figure 7. For rain rates larger than 1 $\mathrm{mm.h^{-1}}$, attenuation is always larger than 3 dB resulting in a possible loss of the signal. The probability of large distortion of the signal (high off-nadir angle or slope) is much lower than the high attenuation one except for very low rain rate (less than 0.5 $\mathrm{mm.h^{-1}}$). Attenuation is thus the most constraining factor. The same analysis was performed for clouds and Figure 8 summarizes the results for the three type of clouds (Gaussian, exponential, constant) and for MODIS high resolution cloud data. For ILWC larger than 1.5 $\mathrm{kg.m^2}$ the signal is always attenuated by more than 3 dB. Distortion has a very low probability for low ILWC and will not be a constraining factor compared to attenuation.

The probability of unavailability of 20 Hz Altika is computed using the probability of large attenuation or strong distortion as a function of rain rate and the rain rate probability from climatology. The rain climatology estimated from dual frequency altimeter missions appears to be the best candidate for such an estimation as it is based on the same physics, i.e. attenuation by rain, and because the data sampling and resolution have similar characteristics than that of the Altika mission. The mean Altika availability is estimated from the Topex/Poseidon rain climatology, i.e.. the rain probability and the rain rate distributions, estimated from 13 years of Topex dual frequency altimeter data [21] (available at *http://cersat.ifremer.fr/fr/data/discovery/by_parameter/altimetry/rain_alt*). The Altika data unavailability (P_u) is estimated as

$$P_u(x,y) = \int_0^\infty P_R(x,y,R)p(R)dR \qquad (13)$$

where $P_R(x,y,R)$ is the probability of rain rate *R* at location (x,y) and $p(R)$ is the probability of unavailability for rain rate *R* (presented in Figure 7).

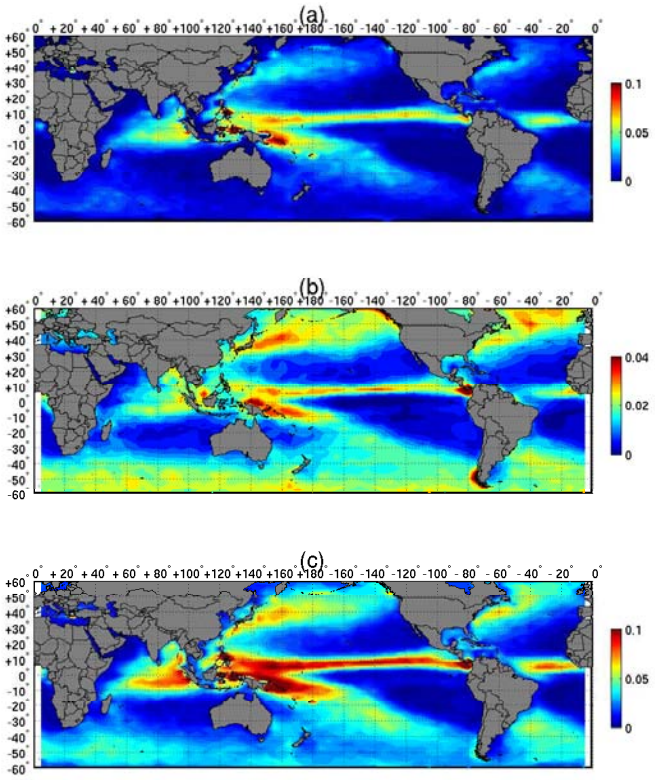

Fig. 9. Mean annual probability of 20 Hz Altika data loss, by rain (a), by cloud liquid water (b) and by rain and clouds (c).

The mean annual unavailability of 20 Hz Altika data presented in Figure 9-a follows the general pattern of the global rain distribution. On a global scale about 2 % of data will be lost, but in the Inter Tropical Convergence Zone and in the Pacific Warm Pool, as much as 8 to 9 % of data will be too attenuated to be processed. About 3 to 4 % of Altika data will be lost in the storm tracks of the North Atlantic and Pacific oceans and in the South Pacific Convergence Zone. Outside these regions about 1 % or less of the data will be strongly affected by rain.

The estimation of the loss of data caused by cloud attenuation requires a climatology of cloud liquid water

content that includes the cloud liquid water distribution and probability. The Level-3 MODIS Atmosphere Monthly Global Products, distributed by NASA at *http://modis-atmos.gsfc.nasa.gov/MOD08_M3*, which contain roughly 800 statistical data sets that are derived from the Level-3 MODIS Atmosphere Daily Global Product, are certainly the best data set to estimate the Altika availability. They contain statistics that are sorted into 1x1 degree cells grid that spans a (calendar) monthly interval. The statistics for a given variable include the histograms of the quantity within each grid box necessary to estimate the unavailability probability using relation (13). The probability $P_L(x, y, ILWC)$ of ILWC at a given location *(x,y)* is estimated as the product of the cloud fraction and the ILWC normalized histograms (or probability density function). Two years of data (2003 and 2004) are used to estimate the mean Altika unavailability.

The mean unavailability of 20 Hz Altika data caused by cloud, presented in Figure 9-b, sensibly differs from that for rain, especially at mid and high latitude. The global mean value is about 1.5 % of loss and the maximum of about 3 to 4 % is reached not only in the Inter Tropical Convergence Zone, the Pacific Warm Pool but also in the storm tracks of the North Atlantic and Pacific oceans and in the South Pacific Convergence Zone. A relative maximum larger than 2 % is also observed in the southern Ocean. Outside these regions, i.e. mainly in the oceanic deserts, less than 1 % of the data will be significantly affected by clouds.

It is a truism to say that there is no rain without clouds and, in principle, the two can not be considered separately as there exists a continuum in the drop size distribution from haze to strong rain. However, in practice it is simpler to consider rain and cloud separately and to add the rain and cloud loss probability to estimate an upper limit of the overall data unavailability. This also allows to take into account very light rain cases that are not very well represented in global rain climatology. The resulting probability presented in Figure 9-c shows that in the Tropics as much as 10-12 % of the data might be lost and about 5 % in oceanic storms tracks. In the remaining oceanic regions the data loss will not exceed 2 %.

B. Availability of 1-sec (GDR) Altika data

Geophysical Data Record (GDR) , i.e. the one second average values of 20-Hz MLE4 geophysical parameters are the most widely used and distributed altimeter data. When an altimeter flies over a rain cell, part of the individual 20 Hz waveforms can be too strongly affected by rain to be processed and should not be used to compute GDR values. For past altimeters such as Jason, the 1-sec GDR data were flagged as erroneous if more than 50 % of the high rate waveforms were flagged. The availability of the GDR data depends thus on the probability of loss of 20-Hz data over 1 second. Figure 10 presents the percentage over 1 second of 20 Hz waveforms for which the attenuation is larger than 3 dB, the off-nadir angle larger than 0.01 deg^2 or the slope larger than 1.2 for Gaussian rain cells as well as the synthesis for the three parameters. The results are given as a function of integrated rain rate and rain cell diameters as this parameter is more explicit when

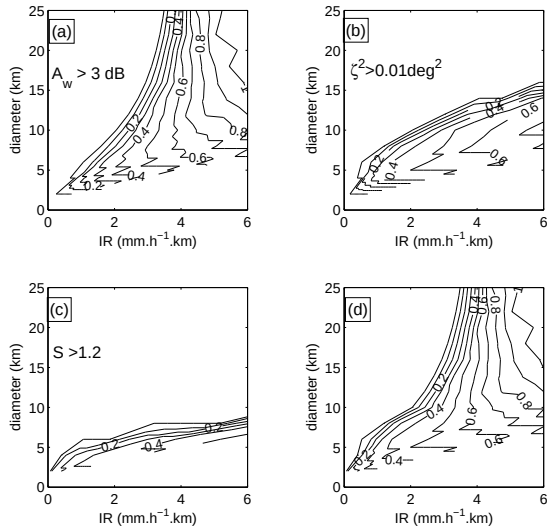

Fig. 10. Percentage over 1 sec of 20 Hz waveforms for which the attenuation is larger than 3 dB (a), off-nadir angle larger than 0.01 deg^2) (b) and slope larger than 1.2 (c) and attenuation or off-nadir angle or slope is too large (d) as a function of rain rate.

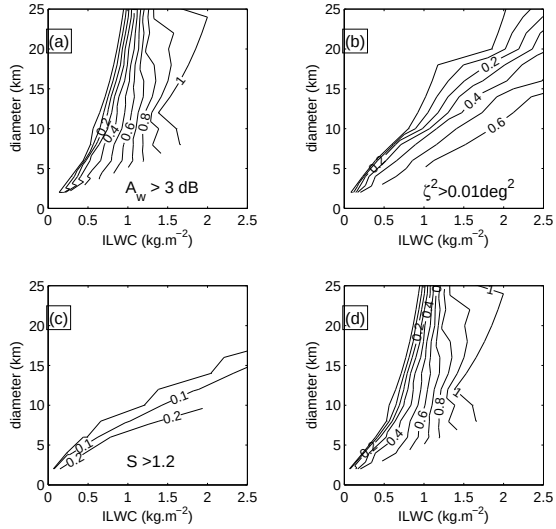

Fig. 11. Percentage over 1 sec of 20 Hz Altika waveforms attenuated by more than 3 dB (a), for which the off-nadir angle is larger than 0.01 deg ^{2} (b), for which the leading edge slope is larger than 1.2 (c), and for which the three parameters are larger than the thresholds as a function of integrated water content.

considering spatial averages. Three cases can be defined from the results,

1) For heavy rain, $\overline{R} > 5$ mm.h^{-1}km and for diameter larger than 12 km, attenuation plays a major role and all the 20-Hz waveforms are attenuated by more than 3 dB resulting in the loss of geophysical data.

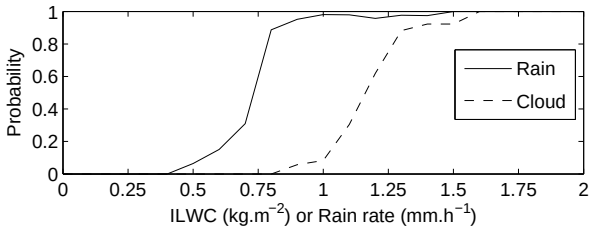

Fig. 12. Probability of having more than 50% of the 20 Hz individual waveforms flagged for high attenuation when averaged over 1 second to compute GDR data.

2) For light rain, $\overline{R} < 3$ mm.h^{-1}km and diameter larger than 10 km, no data are lost and the geophysical data quality will not be affected.
3) For small rain cell, i.e. diameter less than 10 km between 10 to 80 % of 20 Hz data can be lost because of attenuation and/or distortion and it will be of prime importance to accurately flag and eliminate all the waveforms possibly affected by rain to maintain the GDR accuracy.

Similar results were found for exponential and constant rain cells but are not presented here.

The same analysis was conducted for clouds and the results, presented in Figure 11 for Gaussian clouds, are very similar to the ones found for the rain analysis with three cases

1) For dense (high liquid water content) large clouds, $\overline{L} > 1.5\,\mathrm{kg.m}^{-2}$ and diameter >20 km), all the 20-Hz waveforms are attenuated by more than 3 dB resulting in the complete loss of geophysical data.
2) For light and large clouds, $\overline{L} < 1.0\,\mathrm{kg.m}^{-2}$ and diameter >10 km, no waveform are affected and the geophysical data quality should be nominal.
3) For small clouds, i.e. diameter less than 10 km, and moderate to high water content, between 10 to 80% of the 20-Hz data can be lost because of attenuation and/or distortion. The estimation of GDR data can still be possible if the waveforms possibly affected by clouds are correctly eliminated.

The GDR's availability can be estimated from the rain and cloud climatology using relation (13) and the probabilities of having more than 50% of the 20 Hz individual waveform flagged for high attenuation or distortion as a function of rain rate and ILWC. These probabilities, estimated from the model results, are presented in Figure 12. The general patterns of the unavailability fields presented in Figure 13 are very similar to the 20 Hz ones and for rain the values are almost identical to the 20 Hz ones mainly because of the strong attenuation by rain. As expected, they are sensibly lower for clouds and the probability of unavailability of GDR data is almost half that of 20 Hz data. This is particularly true at high latitudes in the southern ocean and within the oceanic storm tracks where less than 2% of the GDR data might be lost.

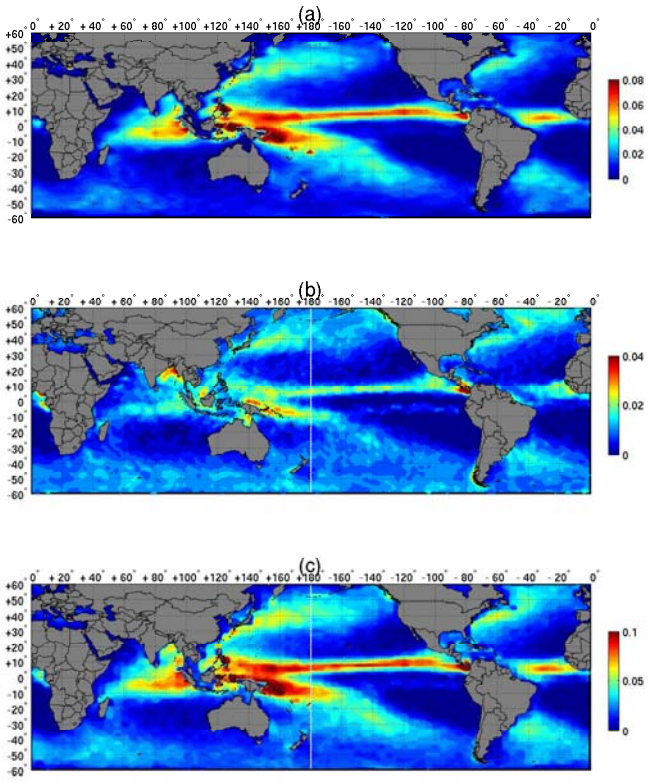

Fig. 13. Mean annual unavailability of GDR Altika data (i.e. more than 50 % of the individual 20 Hz measurement attenuated by more then 3 dB), by rain (a), by cloud liquid water (b) and by rain and clouds (c).

The overall unavailability of GDR data is about 2.5%. So, even if attenuation by atmospheric liquid water is a strong constraint, the data availability should be well above 95%. However, locally, especially in the Tropics, the availability can be less than 90% and for a particular period of the year less than 80-85%.

VI. Summary and Conclusion

The Altika mission, scheduled for launch in 2010, will carry the first Ka-band radar altimeter instrument to be flown in space. The major drawback of the use of Ka-band is the strong attenuation of the signal by atmospheric liquid water associated with cloud or rain. Because of the Altika altimeter design, attenuation of the signal will be a strong limiting constraint on the data availability and signal attenuated by more than 3 dB might be lost (in worst case). It is thus of prime importance to quantify the effects of atmospheric liquid water on altimeter waveforms and geophysical parameter estimates. It is also important to determine the probability of data loss by liquid water.

The model of interaction between atmospheric liquid water and altimeter signal developed originally for Topex/Poseidon has been adapted to the Altika configuration to estimate the effect of rain and clouds on the Altika waveform, in particular

attenuation and waveform distortion. The model has been applied to a wide range of rain cells and clouds and the results show that both attenuation and distortion depend more strongly on the rain (or ILWC) variability within the altimeter footprint than on the mean rain (or ILWC). This brings to light the problem of a pertinent correction using coincident passive microwave estimates of rain rate and ILWC. Furthermore, the results show that the difference between attenuation and one that can be estimated from these passive microwave estimates can exceeds 1 dB even for light rain rate or ILWC if the rain or ILWC variability is high.

The accuracy of geophysical parameter estimates in presence of cloud and rain has been studied by applying the planned retracking algorithm (MLE4) to the ensemble of waveforms simulated in presence of liquid water. The analysis of the bias and standard deviation of the four retrieved parameters, range, swh, backscatter and off-nadir angle, shows that when the distortion is large, mainly for small rain cells and small dense clouds, the range and swh biases and standard deviation's can largely exceeds the altimeter performances specifications. As MLE4 model does not included the atmospheric attenuation by liquid water, it is impossible to estimate the true surface backscatter and off-nadir. However, MLE4 retrieves correctly the apparent off-nadir angle estimated by waveform analysis and overestimates the apparent backscatter. The analysis of the range and swh errors as a function of off-nadir angle and leading edge slope shows that for off-nadir angles larger than 0.01 deg^2 and for leading edge slope larger than 1.2 the accuracy of the retrieved geophysical parameters will not meet the performances specifications. As these range and swh errors are only weakly dependent on rain rate or ILWC, these parameters can certainly not be used to accurately flag the samples potentially affected. This implies that an independent rain/cloud flag will have to be defined to eliminate the data and that it should be based on the analysis of the altimeter signal alone. Part II of the present paper will be devoted to the definition and validation of this new rain/cloud flag.

The model results were also used to compute the mean probability of high attenuation and high distortion as a function of rain rate or ILWC, i.e. the two parameters available in rain and cloud climatology. The 13 year TOPEX/Poseidon rain climatology, which contains rain probability as well as rain rate histograms, is used to estimate the mean unavailability. For 20 Hz Altika data, the overall data loss is about 2 %, but can reach 8-9 % in the Tropics and 4-5 % in the oceanic storm tracks. Two years of MODIS level-3 monthly global cloud products are used to compute the loss of data caused by clouds. About 1 % of the global data will be strongly attenuated by clouds. In the Tropics, the value can reach 4-5 % as well as in the main oceanic storms tracks. On a global scale, about 3.4 % of the 20 Hz Altika data will be lost because of clouds and rain.

Geophysical Data Record data are the main kind of altimeter data distributed to the community. They consist of one second averaged 20 Hz geophysical parameter estimates. They are considered as invalid if more than 50% of the 20-Hz individual estimates are flagged for bad quality. The probability of unavailability of GDR data because of rain is of the same order of magnitude as the 20 Hz data one, i.e. about 2%. However, it is about half that of 20 Hz data when considering cloud attenuation. About 2.5% of the GDR data will be lost because of rain and clouds. If within the tropical band about 10% of the data will be lost, outside this region the unavailability is less than 2 %, except in the storm tracks where it can reach 4%. These values are well within the 90% availability required by the mission specification.

APPENDIX
RAIN CELL AND CLOUD ANALYTICAL MODELS

Three models were used: Gaussian, exponential and constant. Let *Z* be the rain rate, *R*, or the integrated liquid water content, *ILWC*, the Gaussian model is defined for a cell/cloud of diameter d by

$$Z(x,y) = Z_0 e^{-\frac{(x-x_0)^2+(y-y_0)^2}{r^2}} \tag{14}$$

where (x_0, y_0) are the cell center coordinates, and $r = d/(2\sqrt{ln2})$ thus $Z = Z_0/2$ for $\sqrt{(x-x_0)^2+(y-y_0)^2} = d/2$.

An exponential cell/cloud is defined by

$$Z(x,y) = Z_0 e^{-\frac{\left[(x-x_0)^2+(y-y_0)^2\right]^{1/2}}{r}} \tag{15}$$

where $r = d/(2\ln 2)$, and a constant cell/cloud by

$$Z(x,y) = 0 \quad if \quad \sqrt{(x-x_0)^2+(y-y_0)^2} > r \tag{16}$$

$$Z(x,y) = Z \quad if \quad \sqrt{(x-x_0)^2+(y-y_0)^2} <= r \tag{17}$$

where $r = d/2$.

REFERENCES

[1] P. Vincent, N. Steunou, E. Caubet, L. Phalippou, L. Rey, E. Thouvenot, and J. Verron, "AltiKa: a Ka-band Altimetry Payload and System for Operational Altimetry during the GMES Period," *Sensors*, vol. 6, pp. 208-234, 2006.

[2] J. Tournadre, "Estimation of rainfall from ka band altimeter data : computation of waveforms in presence of rain," in *Procs of IGARSS-99, IEEE Press, Piscataway, NJ, Hambourg, Allemagne, 28 juin-2 juil*, vol. I. IEEE Press, 1999, pp. 197-199.

[3] F. Ulaby, R. Moore, and A. Fung, *Microwave remote sensing active and passive: Fundamentals and radiometry*, ARTECH House Norwood MA, Ed. Reading, Massachusetts: Addison-Wesley Publ. Comp., 1981, vol. I.

[4] F. Monaldo, J. Goldhirsh, and E. Walsh, "Altimeter height measurement error introduced by the presence of variable cloud and rain attenuation," *J. Geophys. Res*, vol. 91, pp. 2345-2350, 1986.

[5] G. D. Quartly, T. H. Guymer, and M. A. Srokosz, "The effects of rain on Topex radar altimeter data," *J. Atmos. Oceanic. Tech.*, vol. 13, pp. 1209-1229, 1996.

[6] J. Tournadre and J. C. Morland, "The effects of rain on TOPEX/Poseidon altimeter data," *IEEE Trans. Geosc. Remote Sens.*, vol. 35, no. 5, pp. 1117-1135, Sep. 1997.

[7] J. Tournadre, "Determination of rain cell characteristics from the analysis of Topex altimeter echo waveforms," *J. Atmos. Oceanic Technol.*, vol. 15, no. 2, pp. 387-406, Apr. 1998.

[8] G. D. Quartly, "Determination of Oceanic Rain Rate and Rain Cell Structure from Altimeter Waveform Data. Part I: Theory," *J. Atmos. Oceanic Tech.*, vol. 15, no. 6, pp. 1361-1378, 1998.

[9] F. NouÃ«l, J.-P. Berthias, M. Deleuze, A. Guitart, P. Laudet, A. Piuzzi, D. Pradines, C. Valorge, C. Dejoie, M.-F. Susini, and D. Taburiau, "Precise Centre National d'Etudes Spatiales orbits for TOPEX/Poseidon, Is 2-cm still a challenge?" *J. Geophys. Res. Oceans*, vol. 99, p. 24,405-24,419., 1994.

[10] G. S. Brown, "The average impulse response of a rough surface and its applications," *IEEE Trans. Antennas Propag.*, vol. AP-25, pp. 67-74, 1977.
[11] D. E. Barrick, *Remote Sensing of the Troposphere*. V.E. Derr Ed.,, U.S. Govt. Printing Office, Washington, D.C., 1972, ch. 12 Remote sensing of sea state by radar, pp. 12.1-12.6.
[12] D. Barrick and B. Lipa, "Analysis and interpretation of altimeter sea echo," *Satellite Oceanic Remote Sensing, Advances in Geophysics*, vol. 27, pp. 61-100, 1985.
[13] F. T. Ulaby, R. K. Moore, and A. K. Fung, *Microwave remote sensing: Fundamentals and radiometry*, ARTECH House Norwood MA., Ed. Reading, Ma, USA: Addison-Wesley Publ. Comp., 1981, vol. I.
[14] J. Marshall and W. M. Palmer, "The distribution of raindrops with size," *J. Meteor.*, vol. 5, pp. 165-166, 1948.
[15] J. Goldhirsh and E. Walsh, "Rain measurements from space using a modified seasat-type radar altimeter," *IEEE Trans. Antennas Propag*, vol. AP-30, pp. 726-733, 1982.
[16] R. L. Olsen, D. V. Rogers, and D. B. Hodge, "The aR^b relation in the calculation of rain attenuation," *IEEE Trans. Antennas and Propag.,*, vol. AP-26, pp. 318-329, 1978.
[17] J. Benveniste, Ed., *ENVISAT RA2/MWR Products Handbook*. European Space Agency, ESRIN; Frascati, Italy, no. PO-TN-ESR6RA-0050, 2002.
[18] E. J. Walsh, F. M. Monaldo, and J. Goldhirsh, "Rain and Cloud effects on a satellite dual-frequency radar altimeter system operating at 13.5 and 35 GHz," *IEEE Trans. Geosc. Remote Sens.*, vol. 22, pp. 615-622, 1984.
[19] W. P. Menzel, R. A. Frey, B. A. Baum, and H. Zhang, "Cloud Top Properties and Cloud Phase - Algorithm Theoretical Basis Document. Products: 06-L2, 08-D3, 08-E3, 08-M3," NASA Goddard Space Flight Center, Tech. Rep. ATBD Reference Number: ATBD-MOD-05, 2006.
[20] L. Amarouche, P. Thibaut, O. Zanife, J.-P. Dumont, P. Vincent, and N. Steunou, "Improving the Jason-1 ground retracking to better account for attitude effects," *Marine Geod.*, vol. 27, pp. 171-197, 2004.
[21] J. Tournadre, "Improved level-3 oceanic rainfall retrieval from dual-frequency spaceborne radar altimeter systems," *J. Atmos. Oceanic Technol.*, vol. 23, no. 8, pp. 1131-1149, august 2006.

Jean Tournadre was born in Clermont-Ferrand, France, in 1959. He received the diplôme d'ingénieur from the Ecole Centrale de Lyon, Lyon, France in 1981, the Ph.D. degree in Meteorology from the University Blaise Pascal, Clermont-Ferrand, France in 1984, and the Habilitation á Diriger de Recherches from the UniversitÃ© Pierre and Marie Curie, Paris.

He has been post-doctoral researcher at the Scripps Institution of Oceanography, University of California, San Diego (1984-1986) and visiting scientist at the National Center for Atmospheric Research, Boulder (1987), at the University of Hawaii (1997), and at the University of Tohoku, Sendai, Japan (2003). Since 1987, he is a research scientist with the Institut Français de Recherche pour l'Exploitation de la Mer (French Research Institute for Exploitation of the Sea), Plouzané, France, where he works in the Laboratoire d'Océanographie Spatiale.
His research interests are sea surface temperature, microwave remote sensing of the ocean, especially surface winds and waves, and the interaction between radar signal and precipitation.

Juliette Lambin-Artru received the engineer degree form Ecole Polytechnique, Palaiseau, France in 1997 and the Ph.D. in Geophysics from Institut de Physique du Globe de Paris, Paris, France in 2001.

From 2001 to 2005 she was a Postdoctoral Fellow at the California Institute of Technology, Pasadena, CA. In 2005, she joined the Centre National d'Etudes Spatiales in Toulouse, France, as a mission engineer for oceanography, hydrology and cryosphere. She supervised

Nathalie Steunou was born in France in 1974. She received an Engineer degree from Ecole Nationale de l'Aviation Civile, Toulouse, France in 1996.

In 1996 she joined the Centre National D'Etudes Spatiales (CNES) in Toulouse, France where she works as a radar engineer for altimeters and radiometers oceanographic satellite missions.